Observation of γ vibrations and alignments built on non-ground-state configurations in ^{156}Dy

S. N. T. Majola,[1,2,*] D. J. Hartley,[3] L. L. Riedinger,[4] J. F. Sharpey-Schafer,[5] J. M. Allmond,[6,17] C. Beausang,[6] M. P. Carpenter,[7] C. J. Chiara,[8] N. Cooper,[9] D. Curien,[10] B. J. P. Gall,[10] P. E. Garrett,[11] R. V. F. Janssens,[7] F. G. Kondev,[8] W. D. Kulp,[12] T. Lauritsen,[7] E. A. McCutchan,[7,13] D. Miller,[4] J. Piot,[10] N. Redon,[14] M. A. Riley,[15] J. Simpson,[16] I. Stefanescu,[7] V. Werner,[9] X. Wang,[15] J. L. Wood,[12] C.-H. Yu,[17] and S. Zhu[7]

[1]*iThemba LABS, National Research Foundation, P.O. Box 722, Somerset-West 7129, South Africa*
[2]*Department of Physics, University of Cape Town, P/B X3, Rondebosch 7701, South Africa*
[3]*Department of Physics, U.S. Naval Academy, Annapolis, Maryland 21402, USA*
[4]*Department of Physics, University of Tennessee, Knoxville, Tennessee 37996, USA*
[5]*Department of Physics, University of the Western Cape, P/B X17, Bellville 7535, South Africa*
[6]*Department of Physics, University of Richmond, Richmond, Virginia 23173, USA*
[7]*Physics Division, Argonne National Laboratory, Argonne, Illinois 60439, USA*
[8]*Nuclear Engineering Division, Argonne National Laboratory, Argonne, Illinois 60439, USA*
[9]*Wright Nuclear Structure Laboratory, Yale University, New Haven, Connecticut 06520, USA*
[10]*Université de Strasbourg, IPHC, 23 rue du Loess 67037 Strasbourg, France and CNRS, UMR7178, 67037 Strasbourg, France*
[11]*Department of Physics, University of Guelph, Guelph, Ontario, Canada*
[12]*School of Physics, Georgia Institute of Technology, Atlanta, Georgia 30332, USA*
[13]*National Nuclear Data Center, Brookhaven National Laboratory, Upton, New York 11973, USA*
[14]*Institut de Physique Nucléaire Lyon, IN2P3-CNRS, Lyon, F-69622 Villeurbanne, France*
[15]*Department of Physics, Florida State University, Tallahassee, Florida 32306, USA*
[16]*STFC Daresbury Laboratory, Daresbury, Warrington WA4 4AD, United Kingdom*
[17]*Physics Division, Oak Ridge National Laboratory, Oak Ridge, Tennessee 37831, USA*

(Received 11 December 2014; revised manuscript received 16 February 2015; published 26 March 2015)

The exact nature of the lowest $K^\pi = 2^+$ rotational bands in all deformed nuclei remains obscure. Traditionally they are assumed to be collective vibrations of the nuclear shape in the γ degree of freedom perpendicular to the nuclear symmetry axis. Very few such γ bands have been traced past the usual backbending rotational alignments of high-j nucleons. We have investigated the structure of positive-parity bands in the $N = 90$ nucleus ^{156}Dy, using the ^{148}Nd(^{12}C,4n) ^{156}Dy reaction at 65 MeV, observing the resulting γ-ray transitions with the Gammasphere array. The even- and odd-spin members of the $K^\pi = 2^+\gamma$ band are observed up to 32^+ and 31^+, respectively. This rotational band faithfully tracks the ground-state configuration to the highest spins. The members of a possible γ vibration built on the aligned yrast S band are observed up to spins 28^+ and 27^+. An even-spin positive-parity band, observed up to spin 24^+, is a candidate for an aligned S band built on the seniority-zero configuration of the 0_2^+ state at 676 keV. The crossing of this band with the 0_2^+ band is at $\hbar\omega_c = 0.28(1)$ MeV and is consistent with the configuration of the 0_2^+ band not producing any blocking of the monopole pairing.

DOI: 10.1103/PhysRevC.91.034330 PACS number(s): 27.70.+q, 21.10.Re, 23.20.Lv, 23.20.En

I. INTRODUCTION

The γ degree of freedom, breaking the axial symmetry in quadrupole deformed nuclei, is indispensable in understanding the level structures observed in nuclear spectroscopy. The traditional interpretation [1] of the lowest $K^\pi = 2^+$ rotational bands, that consistently appear in even-even deformed nuclei, has been that they are a shape vibration in the γ degree of freedom perpendicular to the symmetry axis. These bands have both even- (natural parity) and odd-spin (unnatural parity) states and are observed to have very weak $M1$ $\Delta J = 1$ transitions between the even and the odd members of the bands [2]. The signature splitting between the odd and the even spins depends on the nature of the total energy dependence of the nucleus on the shape parameter γ. Extreme scenarios of this dependence are as follows: (a) γ rigid and finite as calculated by Davydov and Filippov [3] and (b) γ soft, calculated by Wilets and Jean [4].

In odd-A nuclei, the single nucleon in a Nilsson orbital $[N,n_z,\Lambda]\Omega$ can couple to the collective motion of the even-even core. When coupling to the $K^\pi = 2^+$ excitations, two rotational bands will result with the K quantum numbers (angular momentum projection on the symmetry axis) coupled either parallel or antiparallel; thus $K_> = (\Omega + 2)$ and $K_< = |\Omega - 2|$. Examples of such couplings have been observed in ^{165}Ho and ^{167}Er [5] and in ^{155}Gd [6,7]. A notable feature of γ bands is that they track the intrinsic configuration, usually the ground state, on which they are based [8,9].

To date there are few examples of γ bands extended to high spins. This is, no doubt, due to these γ bands lying about 1 MeV above the yrast line in most nuclei and therefore only weakly populated in most fusion-evaporation reactions. In Table I we list examples of even-even nuclei in which the γ band has been observed up to spins higher than $15\hbar$.

To our knowledge, the first example of a γ vibration, built on an $i^2_{13/2}$ aligned neutron S band, which was observed

*majola@tlabs.ac.za

TABLE I. Some even-even nuclei in which the γ band has been observed above spin 15^+.

Nucleus	Beam species	Energy (MeV)	Highest spin reached			Reference
			Yrast band	γ even	γ odd	
^{104}Mo[a]	ff		20^+	18^+	17^+	[13]
^{154}Gd	α	45	24^+	16^+	17^+	[14]
^{156}Dy	^{12}C	65	32^+	32^+	31^+	This paper
^{160}Dy	^{7}Li	56	28^+	22^+	25^+	[15]
^{162}Dy[b]	^{118}Sn	780 Coulex	24^+	18^+	17^+	[16]
^{162}Dy	^{7}Li	56	28^+	18^+	17^+	[15]
^{164}Dy[b]	^{118}Sn	780 Coulex	22^+	18^+	11^+	[16]
^{156}Er	^{48}Ca	215	26^+	26^+	15^+	[12]
^{160}Er	^{48}Ca	215	50^+		43^+	[9]
^{164}Er	^{9}Be	59	24^+	14^+	19^+	[17]
^{164}Er	^{18}O	70	24^+	18^+	21^+	[10,11]
^{170}Er	^{238}U	1358 Coulex	26^+	18^+	19^+	[18]
^{180}Hf	^{136}Xe	750 Coulex	18^+	16^+	13^+	[19]
^{238}U	^{209}Bi	1130 and 1330 Coulex	30^+	26^+	27^+	[20]

[a]Fission fragment.
[b]Inverse reaction

beyond the first backbend, was in ^{164}Er [10,11]. In ^{156}Er, the positive-parity members of the γ band are known through the backbend up to $26\hbar$ [12]. In ^{160}Er, the odd-spin members of the γ band are observed through both the $i^2_{13/2}$ neutron alignment and the $h^2_{11/2}$ proton alignment up to spin $43\hbar$ [9]. It appears that, regardless of the underlying microscopic configurations involved in the γ bands, they do not seem to be affected by the orbitals responsible for causing the alignments.

Early microscopic models of collective vibrations in deformed nuclei [21–25] assumed the existence of a vibrational "phonon" or "boson" and then constructed this entity out of some set of basis states. This is accomplished by postulating an interaction, expanding the collective phonon in a truncated basis, and then using the variational principle to minimize the phonon energy in terms of the interaction parameters. An extensive literature exists that discusses optimization of bases, truncations, and fitting the parameters. Phenomenological models, such as the interacting boson approximation [26] and geometric approaches [27], suffer from the disadvantage that they say nothing about the underlying microscopic configurations, unlike random-phase approximation calculations that appear to provide a better description [28–31]. The recent triaxial projected shell-model calculations [32–36] seem to give a real hope of obtaining a clear microscopic and physically accurate picture of γ vibrations of deformed nuclei. Reference [35] provides a clear history of approaches to descriptions of γ vibrations.

In this paper, we investigate the positive-parity medium-spin structure of ^{156}Dy and interpret the data in terms of aligned bands and γ vibrations.

II. EXPERIMENTAL DETAILS AND ANALYSIS

We have used the ^{148}Nd(^{12}C,4n) ^{156}Dy reaction with a 65-MeV ^{12}C beam from the Argonne National Laboratory ATLAS accelerator facility to populate excited states in ^{156}Dy. The target was 1.5 mg cm^{-2} of ^{148}Nd with a 1.6 mg cm^{-2} layer of natural Pb evaporated on the back and a 1.5 μg cm^{-2} flash of Au evaporated on the front surface. The Pb layer was to ensure that products from fusion-evaporation reactions stopped in the target. The Au layer was to reduce oxidation of the target while being loaded into the target chamber. The Gammasphere spectrometer [37], consisting of 100 HPGe detectors, each in its own bismuth germinate escape suppression shield, was used with a trigger accepting $\gamma\gamma\gamma$ and higher coincidences. The sorting of the data resulted in $2.05 \times 10^9 \gamma\gamma\gamma$ (or higher-fold) coincident events formed into a standard cube that was analyzed using the RADWARE suite of programs [38].

Although the data were of high statistical quality, they did suffer from over 40 contaminant reactions, both prompt and β-decay delayed. These were as follows:

(i) The (^{12}C,$x\alpha yn$) reactions arising from the fact that ^{12}C is easily split into three α particles by collisions with the target.
(ii) Reactions on the ^{16}O arising from both the Nd target and the Pb backing having significant amounts of oxidation. The γ rays from these reactions are Doppler broadened with widths of up to 100 keV, and this affects gates set on higher-energy γ rays between 1 and 2 MeV.
(iii) The reactions from the 65 MeV ^{12}C beam that was just above the Coulomb barrier for the Pb isotopes. This produced some reaction γ rays and significant amounts of γ rays from the β decays of the products.

The spin and parity assignments of the levels are based on spin-parity selection rules for low-multipolarity γ-ray transitions, the directional correlation from orientated states (DCO) method [39], and the mixing of levels of the same spin parity that lie energetically close to each other. The angular intensity ratio for the Gammasphere in this experiment is as follows:

$$R_{\rm DCO} = I_{\gamma 1}(\text{near } 30^\circ\text{: gated on } \gamma_2 \text{ near } 90^\circ)/I_{\gamma 1} \times (\text{near } 90^\circ\text{: gated on } \gamma_2 \text{ near } 30^\circ).$$

TABLE II. γ-ray E_γ(keV) and level energies E_x(keV) of bands shown in Fig. 1 together with angular intensity ratios $R_{\rm DCO}$ for some of the transitions. Blank entries indicate information that could not be obtained.

E_x (keV)	E_γ (keV)[a]	Multipolarity	I_i^Π	I_f^Π	Band$_f$	$R_{\rm DCO}$
			Ground			
138	137.6	$E2$	2^+	0^+	Ground	0.95(1)
404	266.2	$E2$	4^+	2^+	Ground	0.991(3)
770	366.1	$E2$	6^+	4^+	Ground	1.000(1)
1215	445.1	$E2$	8^+	6^+	Ground	
1724	508.9	$E2$	10^+	8^+	Ground	
2284	560.7	$E2$	12^+	10^+	Ground	
2886	601.8	$E2$	14^+	12^+	Ground	
3522	458.2	$E2$	16^+	14^+	S band	
	635.4	$E2$	16^+	14^+	Ground	
4177	655.1	$E2$	18^+	16^+	Ground	
	679.2	$E2$	18^+	16^+	S band	
4858	680.6	$E2$	20^+	18^+	Ground	
	834.2	$E2$	20^+	18^+	S band	
5571	713.6	$E2$	22^+	20^+	Ground	
6327	756.1	$E2$	24^+	22^+	Ground	
7129	802.1	$E2$	26^+	24^+	Ground	
7977	847.3	$E2$	28^+	26^+	Ground	
			Band 12			
4157	636.4	$M1/E2$	16^+	16^+	Ground	
	1270.3	$E2$	16^+	14^+	Ground	0.89(7)
4697	520.2	$M1/E2$	18^+	18^+	Ground	
	540.4	$E2$	18^+	16^+	Band 12	
	586.4	$E2$	18^+	16^+	Even γ	
	1175.8	$E2$	18^+	16^+	Ground	1.09(11)
5309	451.1	$M1/E2$	20^+	20^+	Ground	
	611.1	$E2$	20^+	18^+	Band 12	
	1132.3	$E2$	20^+	18^+	Ground	0.89(7)
5983	674.5	$E2$	22^+	20^+	Band 12	
	1125.5	$E2$	22^+	20^+	Ground	
6721	737.2	$E2$	24^+	22^+	Band 12	
7519	798.2	$E2$	26^+	24^+	Band 12	
8369	849.7	$E2$	28^+	26^+	Band 12	
			Second vacuum (SV)			
828	424.1	$E2$	2^+	4^+	Ground	0.98(2)
	690.7	$M1/E2$	2^+	2^+	Ground	
1088	259.5	$E2$	4^+	2^+	SV	
	317.7	$E2$	4^+	6^+	Ground	
	683.8	$M1/E2$	4^+	4^+	Ground	
	950.4	$E2$	4^+	2^+	Ground	
1437	348.8	$E2$	6^+	4^+	SV	0.981(3)
	666.7	$M1/E2$	6^+	6^+	Ground	0.682(3)
	1032.9	$E2$	6^+	4^+	Ground	
1858	421.3	$E2$	8^+	6^+	SV	
	642.9	$M1/E2$	8^+	8^+	Ground	0.712(3)
	1088.1	$E2$	8^+	6^+	Ground	
2315	456.6	$E2$	10^+	8^+	SV	
	590.7	$M1/E2$	10^+	10^+	Ground	0.71(1)
	1099.7	$E2$	10^+	8^+	Ground	
			S band			
2706	258.8	$E2$	12^+	10^+	Odd γ	
	390.9	$E2$	12^+	10^+	SV	
	981.7	$E2$	12^+	10^+	Ground	
3065	359.1	$E2$	14^+	12^+	S band	1.000(3)
	780.3	$E2$	14^+	12^+	Ground	
3497	432.7	$E2$	16^+	14^+	S band	
	611.2	$E2$	16^+	14^+	Ground	
	502.5	$E2$	18^+	16^+	S band	
	526.9	$E2$	18^+	16^+	S band	
4634	609.5	$E2$	20^+	18^+	S band	
5319	684.7	$E2$	22^+	20^+	S band	
6069	750.1	$E2$	24^+	22^+	S band	
6876	807.6	$E2$	26^+	24^+	S band	
7737	861.2	$E2$	28^+	26^+	S band	
8649	912.1	$E2$	30^+	28^+	S band	
			Odd-spin γ band (Odd γ)			
1022	617.7	$M1/E2$	3^+	4^+	Ground	
	884.3	$M1/E2$	3^+	2^+	Ground	
1335	312.9	$E2$	5^+	3^+	Odd γ	
	565.4	$M1/E2$	5^+	6^+	Ground	
	931.1	$M1/E2$	5^+	4^+	Ground	
1728	393.1	$E2$	7^+	5^+	Odd γ	
	512.4	$M1/E2$	7^+	8^+	Ground	
	958.1	$M1/E2$	7^+	6^+	Ground	
2190	462.5	$E2$	9^+	7^+	Odd γ	
	466.5	$M1/E2$	9^+	10^+	Ground	
	975.4	$M1/E2$	9^+	8^+	Ground	
	520.1	$E2$	11^+	9^+	Odd γ	
	986.6	$M1/E2$	11^+	10^+	Ground	
3274	563.1	$E2$	13^+	11^+	Odd γ	
3274	989.2	$M1/E2$	13^+	12^+	Ground	
3861	587.2	$E2$	15^+	13^+	Odd γ	
	794.4	$M1/E2$	15^+	14^+	SV	
4457	595.7	$E2$	17^+	15^+	Odd γ	0.902(12)
4457	959.3	$M1/E2$	17^+	16^+	SV	
5079	443.7	$M1/E2$	19^+	18^+	Even γ	
	610.3	$M1/E2$	19^+	17^+	Band 20	
	621.8	$E2$	20^+	18^+	Odd γ	
	1055.3	$M1/E2$	20^+	18^+	S band	
5754	436.1	$M1/E2$	21^+	20^+	Odd γ	
	676.5	$E2$	21^+	19^+	Odd γ	
	690.1	$E2$	21^+	19^+	Band 20	
	1120.3	$M1/E2$	21^+	20^+	S band	
6484	414.1	$M1/E2$	23^+	22^+	Odd γ	
	729.5	$E2$	23^+	21^+	Odd γ	
	1164.9	$M1/E2$	23^+	22^+	S band	
7254	769.5	$E2$	25^+	23^+	Odd γ	
8066	811.2	$E2$	27^+	25^+	Odd γ	
8933	865.5	$E2$	29^+	27^+	Odd γ	
9860	926.9	$E2$	31^+	29^+	Odd γ	
			Even-spin γ band (Even γ)			
890	752.4	$M1/E2$	2^+	2^+	Ground	
1168	277.2	$E2$	4^+	2^+	Even γ	
	763.9	$M1/E2$	4^+	4^+	Ground	
	1030.4	$E2$	4^+	2^+	Ground	
1524	356.5	$E2$	6^+	4^+	Even γ	
	754.5	$M1/E2$	6^+	6^+	Ground	
	1120.6	$E2$	6^+	4^+	Ground	
1956	431.9	$E2$	8^+	6^+	Even γ	
	741.1	$M1/E2$	8^+	8^+	Ground	
	1186.3	$E2$	8^+	6^+	Ground	

TABLE II. (*Continued*.)

E_x (keV)	E_γ (keV)[a]	Multipolarity	I_i^Π	I_f^Π	Band$_f$	R_{DCO}
2447	490.5	$E2$	10^+	8^+	Even γ	
	722.7	$M1/E2$	10^+	10^+	Ground	
	1231.5	$E2$	10^+	8^+	Ground	
2969	522.1	$E2$	12^+	10^+	Even γ	
	682.9	$M1/E2$	12^+	12^+	Ground	
	1245.1	$E2$	12^+	10^+	Ground	
3523	555.7	$E2$	14^+	12^+	Even γ	
	638.1	$M1/E2$	14^+	14^+	Ground	
	1238.2	$E2$	14^+	12^+	Ground	
4110	587.3	$E2$	16^+	14^+	Even γ	0.99(1)
	589.2	$E2$	16^+	16^+	Ground	
	1223.1	$E2$	16^+	14^+	Ground	
4731	553.9	$M1/E2$	18^+	18^+	Ground	
	573.3	$E2$	18^+	16^+	Band 12	
	619.4	$E2$	18^+	16^+	Even γ	
	1209.1	$E2$	18^+	16^+	Ground	
5377	646.1	$E2$	20^+	18^+	Even γ	
6072	695.5	$E2$	22^+	20^+	Ground	
6815	743.2	$E2$	24^+	22^+	Even γ	
7605	790.3	$E2$	26^+	24^+	Even γ	
8445	839.9	$E2$	28^+	26^+	Even γ	
9331	886.2	$E2$	30^+	28^+	Even γ	
10257	926.12	$E2$	32^+	30^+	Even γ	
			Band 17			
3173	467.6	$M1/E2$	12^+	12^+	S band	
	858.2	$E2$	12^+	10^+	SV	
	889.7	$M1/E2$	12^+	12^+	Ground	
	1449.1	$E2$	12^+	10^+	Ground	
3577	404.5	$E2$	14^+	12^+	Band 17	
	511.7	$M1/E2$	14^+	14^+	S band	0.72(2)
	872.5	$E2$	14^+	12^+	S band	0.94(9)
4064	487.1	$E2$	16^+	14^+	Band 17	
	1000.1	$E2$	16^+	14^+	S band	0.95(6)
4617	552.6	$E2$	18^+	16^+	Band 17	
	1120.1	$E2$	18^+	16^+	S band	
5222	604.5	$E2$	20^+	18^+	Band 17	
	1197.1	$E2$	20^+	18^+	S band	
5874	652.8	$E2$	22^+	20^+	Band 17	
	1240.2	$E2$	22^+	20^+	S band	
6577	703.1	$E2$	24^+	22^+	Band 17	
			Band 20			
3942	877.3	$M1/E2$	15^+	14^+	S band	
4468	526.9	$E2$	17^+	15^+	Band 20	
	609.5	$M1/E2$	17^+	16^+	S band	
	970.7	$E2$	17^+	15^+	Odd γ	
5064	597.4	$E2$	19^+	17^+	Band 20	0.97(2)
	606.8	$E2$	19^+	17^+	Odd γ	
	1039.7	$M1/E2$	19^+	18^+	S band	
5710	645.9	$E2$	21^+	19^+	Band 20	1.01(1)
5710	1076.1	$M1/E2$	21^+	20^+	S band	
6409	698.7	$E2$	23^+	21^+	Band 20	0.95(6)
	1091.1	$M1/E2$	23^+	22^+	S band	
7165	753.8	$E2$	25^+	23^+	Band 20	
	1097.3	$M1/E2$	25^+	24^+	S band	
7975	810.5	$E2$	27^+	25^+	Band 20	

[a]The γ-ray energies are estimated to be accurate to ± 0.3 keV.

For stretched transitions, that is $J \rightarrow (J - \lambda)$, where λ is the multipolarity of the γ ray, we expect $R_{DCO} \approx 1$ and $R_{DCO} \approx 0.6$ for $E2$ and dipole transitions, respectively, when they are gated by γ_2 that is a stretched $E2$. If the gating γ_2 is a stretched dipole transition, then we expect $R_{DCO} \approx 1$ and $R_{DCO} \approx 1.5$ for γ_1 being a dipole and $E2$, respectively. If the transitions are not stretched, or have finite $M1/E2$ mixing ratios, the situation is more complicated [40]. To determine parities, conversion coefficients or γ-ray polarization measurements are required [41]. The full set of DCO ratios are given in Table II together with γ-ray and level energies measured in this study.

The partial level scheme of ^{156}Dy, showing the new positive-parity bands discussed in this paper, is displayed in Fig. 1. The bands are labeled using the notation of Ref. [42], the new bands 12, 17, and 20 being labeled in the order in which they were discovered. To identify levels on top of the new positive-parity bands found in this experiment, a previous data set was examined [43] that had used the ^{124}Sn(^{36}S,4n) ^{156}Dy reaction, which transfers more angular momentum in the compound system than the present experiment. The current level scheme further confirms and strengthens the placements of the structures that have been proposed by previous in-beam work [44,45] from low to high spins, and it contributes mostly to nonyrast states in the medium- to high-spin range.

III. EXPERIMENTAL RESULTS

A. The ground-state band

We observe the ground-state rotational band up to the 28^+ state as shown in Fig. 1. Previous experiments using the ^{124}Sn(^{36}S,4n) ^{156}Dy reaction [43] have firmly established this band up to spin 58^+. We observe three new γ rays decaying out of this band at 458, 679, and 834 keV from the 18^+, 20^+, and 22^+ levels, respectively. These feed the yrast aligned S band where these bands cross.

B. The $\nu(i_{13/2})^2$ aligned S band

This band was first observed by Andrews *et al.* [46] and becomes the yrast band at spin 16^+. At spin 12^+ it crosses the rotational band based on the 676 keV 0_2^+ band head. New decays of 503 keV are observed from the 18^+ level to the ground-state band and of 259 keV from the 12^+ level to the 10^+ state in the even-γ band (Fig. 1 and Table II). We observe the S band up to spin 30^+, and it has been firmly identified up to spin 58^+ [43].

C. γ-band extensions

The current experiment confirms all the transitions that have been previously observed [44,45] up to spins 10 and 15 in both the even- and the odd-spin γ bands, respectively. In addition, the even-spin sequence of the γ band has been extended by nine in-band transitions up to 28^+, whereas its odd-spin counterpart has six new transitions up to 27^+. The R_{DCO} values were measured for some of the in-band members where possible, and they are consistent with an $E2$ character

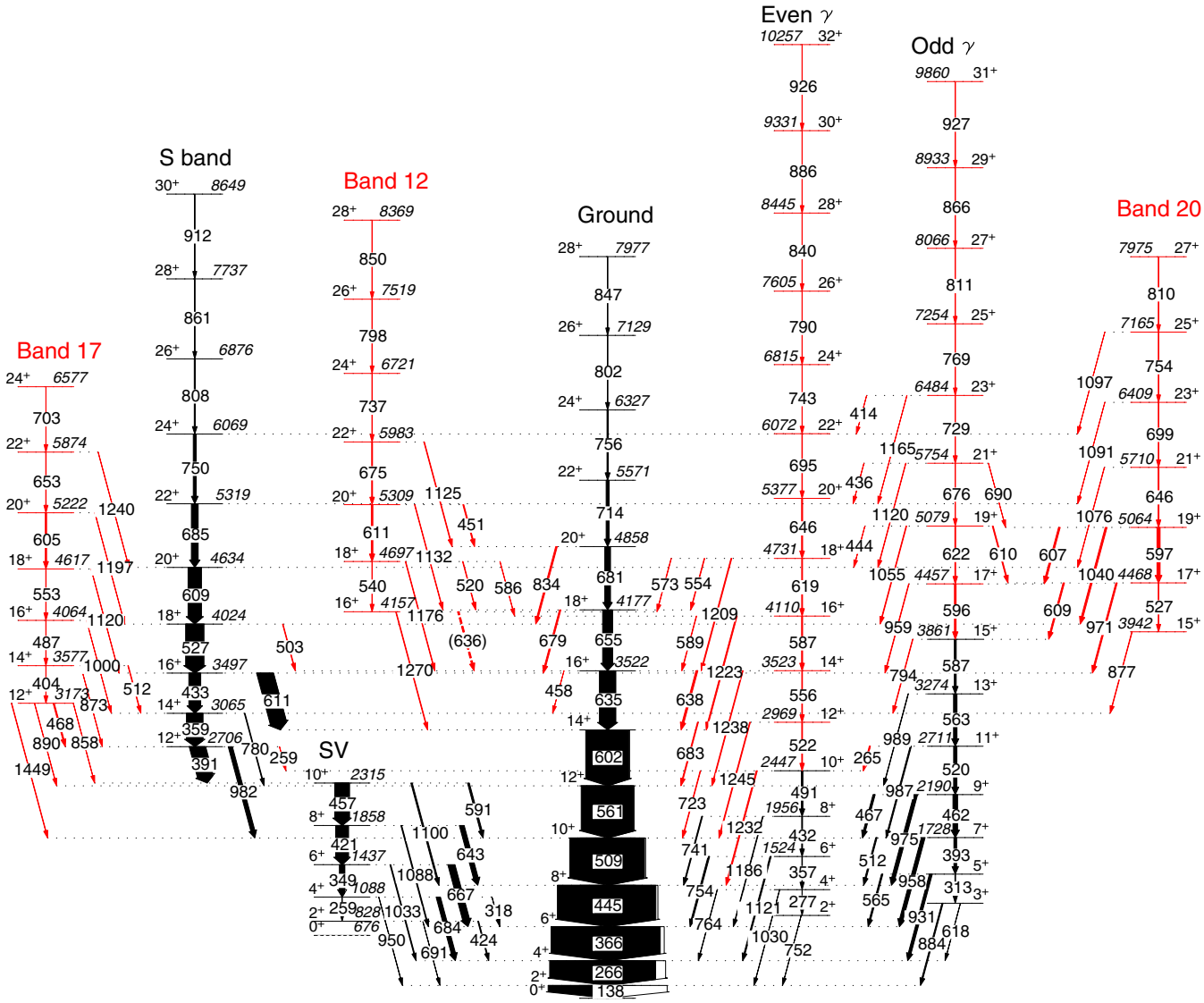

FIG. 1. (Color online) Partial level scheme deduced for ^{156}Dy from the current paper for positive-parity states. New levels and γ-ray transitions are shown in red whereas their known counterparts from previous in-beam work are shown in black. The widths of the arrows are proportional to the intensities of the transitions.

(Table II). Moreover, to further complement the high-spin structures of these states, the ^{36}S-induced reaction data have been reanalyzed. The data for this experiment were collected more than a decade ago by Kondev *et al.* [43]. These data have good statistics and not only enabled us to confirm the high-spin states on the γ bands, observed in the present experiment, but also allowed us to further extend the γ bands by two levels for both the even- and the odd-spin γ sequences. Figures 2(a) and 2(b) show the spectra that were used to establish new in-band members of both the even- and the odd-spin sequences of the γ bands. The insets in both Figs. 2(a) and 2(b), labeled as (i) and (ii), show spectra from the ^{36}S-induced reaction for both the even- and the odd-spin sequences, respectively. The spin and parity assignments for the new levels at 32^+ and 31^+ are based on the assumption that these additional levels are connected by stretched $E2$ transitions. The extensions that have been performed on these sequences from the current analysis mark the highest spin ever to be observed for both the even- and the odd-spin γ bands in any nucleus.

D. New positive-parity bands

1. Band 12

Band 12 is a new structure that has been established from this paper using the carbon-induced reaction. A representative spectrum showing some of the in-band members of band 12 is presented in Fig. 3(a). This rotational sequence consists of six in-band transitions. The main intensity of this band flows through high-energy 1125, 1132, 1176, and 1270 keV out-of-band transitions that populate the ground-state band (Fig. 1). The $R_{\rm DCO}$ values for these high-energy transitions were found to be close to 1 (Table II), and this implies that they are likely to be stretched $E2$ transitions or unstretched $E1$ transitions. If these γ rays are assigned as unstretched $E1$

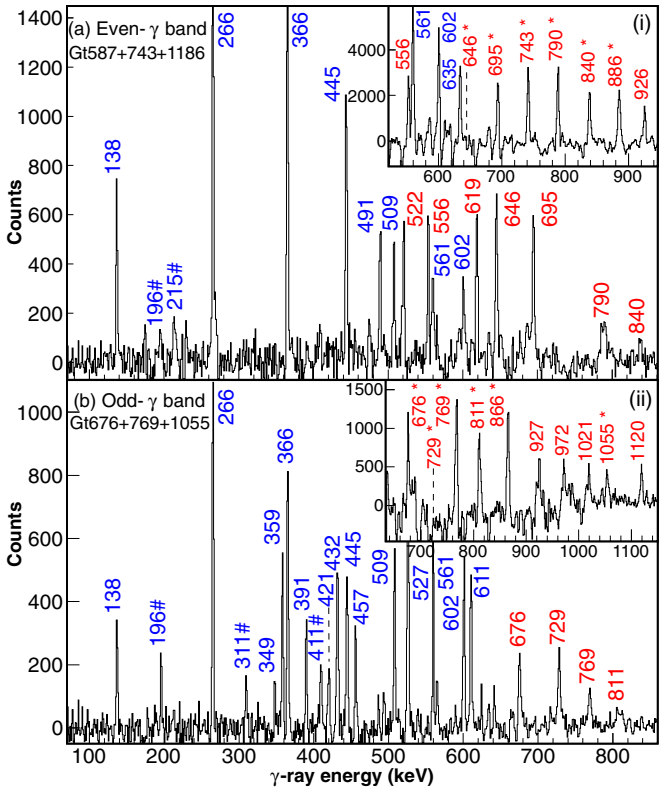

FIG. 2. (Color online) Summed coincident spectra for the (a) even-spin and (b) odd-spin members of the γ bands obtained from the ^{12}C- and ^{36}S- [insets (i) and (ii)] induced reactions. New transitions are colored in red whereas contaminants are denoted by hash (#) symbols. In the insets (i) and (ii), transitions marked by asterisks (*) were included in the gating that produced the coincident spectra.

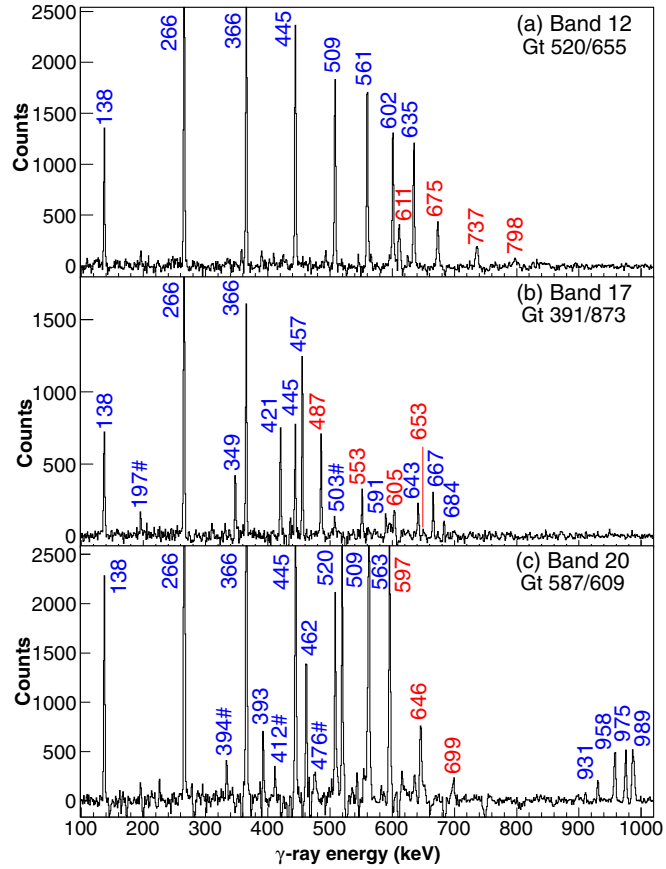

FIG. 3. (Color online) (a)–(c) Summed coincident spectra for bands 12, 17, and 20, respectively, obtained from the ^{12}C data. Transitions corresponding to these newly found structures are labeled in red whereas contaminants are denoted by hash (#) symbols.

transitions, it would mean that the other out-of-band 451, 520, and 636 keV γ rays are $M2$ transitions, and this is considered very unlikely. Therefore, we conclude that these high-energy transitions are stretched $E2$ transitions. This gives spin-parity assignments of 16^+, 18^+, 20^+, 22^+, 24^+, 26^+, and 28^+ to the 4157, 4697, 5309, 5983, 6721, 7519, and 8369 keV levels of band 12, respectively. Furthermore, the energies of the 16^+ states of this band and the even-γ band are close in energy (i.e., 4157 and 4110 keV, respectively). The interlinking 586 and 573 keV $E2$ transitions that connect these two bands indicate that there is a mixing between these bands at this spin 16. This is only possible if these bands are of the same spin parity, and this confirms our spin and parity assignments.

2. *Band 17*

Band 17 is a new band that decays mainly to the S band (Fig. 1). The DCO ratios of the 873 and 1000 keV transitions feeding the 12^+ and 14^+ members of the S band show stretched $E2$ character (Table II) highly favoring the 3577 and 4064 keV members of band 17 to be 14^+ and 16^+, respectively. Again, if these transitions were to be assigned as unstretched $E1$ transitions, it would mean that the other out-of-band 512, 468, and 890 keV transitions are $M2$ transitions, and this is very unlikely. The assignments of the rest of the levels are based on the assumption that they are band members of band 17 connected by in-band $E2$ transitions. A coincidence spectrum illustrating the photopeaks corresponding to the in-band members of this structure is shown in Fig. 3(b).

3. *Band 20*

A previously unobserved sequence of seven levels based upon the state at 3942 keV has been established and is labeled as band 20 in this paper. This band is also among the newly identified medium-spin structures that decay predominantly to the S band via a series of high-energy transitions. It also decays to the 17^+ and 15^+ members of the odd-spin γ band via almost degenerate 607 and 609 keV transitions, respectively. The DCO measurements for the majority of the in-band members of this structure are consistent with them being stretched $E2$ transitions. At spin 17^+, cross transitions link the odd-spin γ band and band 20 from almost energy degenerate states (i.e., separated by less than 20 keV). The identification of the interconnecting transitions between sequences of the same parity and signature confirm and strengthen the proposed assignments. A double-gated spectrum showing some of the in-band members of this structure is shown in Fig. 3(c).

IV. DISCUSSION

A. The 0_2^+ pairing isomer state at 676 keV

Recent work has shown that the first excited 0_2^+ states in $N = 88$ and 90 nuclei are not β vibrations [47] but have properties resembling pairing isomers [48] and are states lowered into the pairing gap by configuration-dependent pairing [14,49]. They are neutron 2p-2h seniority-zero states formed by raising two neutrons out of the ground-state configuration into the $\nu h_{11/2}[505]11/2^-$ Nilsson orbit. This orbit is raised from the lower filled shell to the Fermi surface at the onset of deformation after the $N = 82$ shell closure. Pairs of neutrons in this high-K "oblate" polar orbit do not take part in the normal monopole pairing produced by the high density of low-Ω "prolate" equatorial rotationally aligned orbitals [50]. Due to the small overlap of the wave functions of prolate and oblate single-particle states, $[505]^2$ configurations are decoupled from the pairing involved in the alignment of low$-\Omega$ $i_{13/2}$ neutrons that cause backbending in the rotational bands of deformed nuclei near $N = 90$ [51]. The first excited 0_2^+ states in $N = 88$ and 90 nuclei are then seniority-zero states. These 0_2^+ states may be viewed as a second vacuum [14,49] on which excited states are built that are congruent to the excited states built on the ground-state vacuum. We will refer to the rotational band built on the 0_2^+ state at 676 keV in ^{156}Dy as the SV band.

As observed by Andrews *et al.* [46], this SV band is crossed by the S band at spin 12^+ and at a rotational frequency of $\sim$200 keV compared to the usual $i_{13/2}$ neutron alignment frequency $\hbar\omega_c \approx 280$ keV [52]. This crossing is just a simple band crossing and has nothing to do with the cranked shell model [53] AB-band crossings [54] where the Coriolis force exceeds the monopole pairing energy.

B. The $K^\pi = 2^+\gamma$ bands

In Fig. 4 we show the excitation energies E_x minus a rotational energy $E_R = 7.7I(I+1)$ MeV for the positive-parity states that we observe (Fig. 1) in ^{156}Dy. In Fig. 5(a) we show the alignment $i_x = I_x(\omega) - I_{x,\mathrm{ref}}(\omega)$ of these bands plotted against rotational frequency $\hbar\omega$. In Fig. 5(b) we show

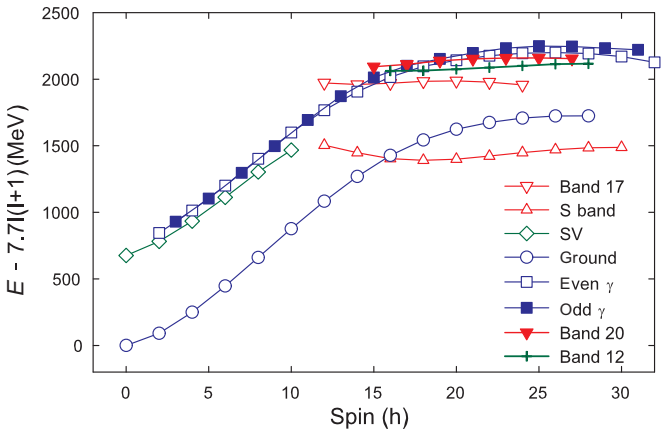

FIG. 4. (Color online) Plot of the excitation energy minus a rigid rotor for the positive-parity bands shown in Fig. 1.

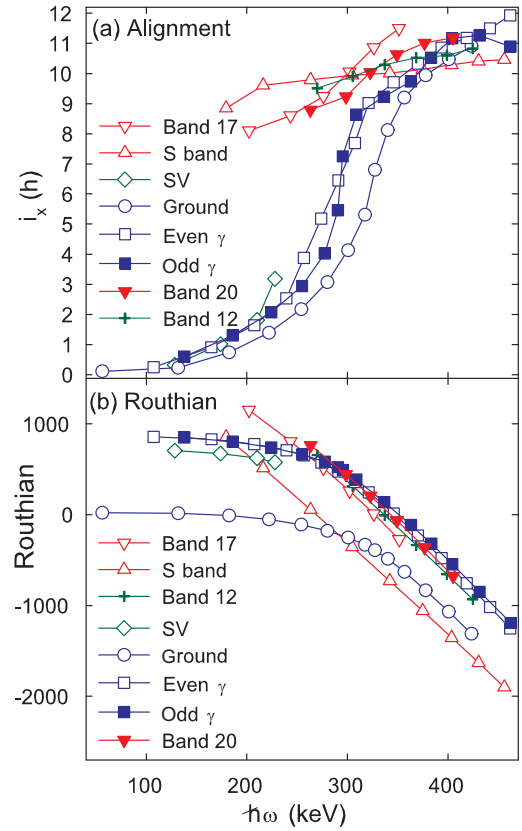

FIG. 5. (Color online) (a) and (b) Plots of alignment i_x and Routhians e', respectively, for the positive-parity bands in ^{156}Dy.

the energies, e' Routhians [53], in the rotating frame for these bands, again as a function of $\hbar\omega$.

It can be seen from Fig. 4 that both the even- and the odd-spin γ bands track parallel to the ground-state band faithfully all the way to spin 32^+. This is very similar to the observation of Ollier *et al.* [9] who find the odd-spin γ band in ^{160}Er to track parallel to the yrast band through both the first backbend, $i_{13/2}$ neutron alignment, and then the second up bend, $h_{11/2}$ proton alignment. In Fig. 5(a), where the alignment i_x is plotted against rotational frequency $\hbar\omega_c$, it can be seen that the alignment in the γ bands comes at a slightly lower frequency than in the ground-state band. This has been explained by Yates *et al.* [11] as a geometrical effect due to the additional excitation energies of the γ bands and the aligned $i_{13/2}$ neutron bands based on the γ bands.

The even-spin members of the γ band in ^{156}Dy have more neighboring bands of the same spin parity than the odd-spin members of the γ band. Hence we would expect there to be more band mixing affecting the excitation energies of the positive-parity states than odd-spin positive-parity bands disturbing the energies of the odd-spin states. It can be seen from Fig. 4 that there is no signature splitting in the γ bands up to spin 12^+, after which there is a very small signature splitting where the even-spin states lie below the odd-spin states. This could be due to either different band mixing or a change in the γ deformation. The absence of signature splitting is an indication that there is no γ deformation so that the nucleus is axially symmetric.

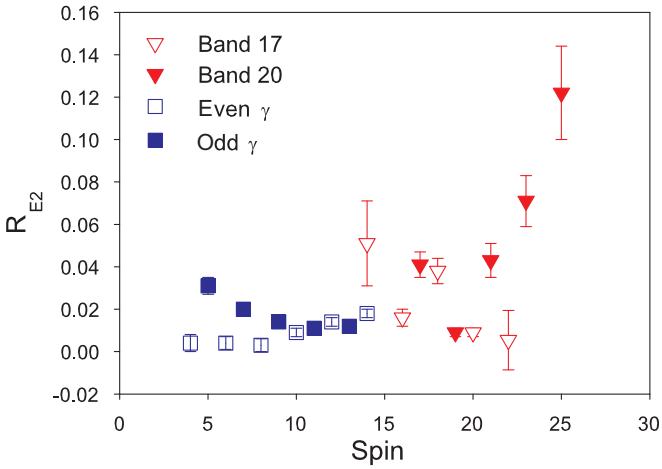

FIG. 6. (Color online) Ratios of the $B(E2)$ values for out-of-band to in-band transitions $R_{E2} = B(E2;\text{out})/B(E2;\text{in})$ for the γ decays from the γ bands to the ground-state band with the γ decays from bands 17 and 20 to the S band. It is assumed that the out-of-band $J \rightarrow (J-1)$ transitions are dominated by the $E2$ component due to the $\Delta K = 2$ nature of γ band to ground-state band transitions, so we have neglected any $M1$ components.

C. Bands 17 and 20

Both band 17 and band 20 decay mainly to the yrast S band. The exceptions are two transitions to the ground-state band out of the lowest, 12^+ state of band 17, and where band 20 crosses the odd-spin γ band between spins 17^+ and 21^+. This strongly preferred decay pattern suggests that these two bands are closely connected to the S band. Indeed, Fig. 5(a) shows that both band 17 and band 20 have alignments close to $10\hbar$. We suggest that band 17 and band 20 could be bands formed by a γ vibration built on the S band configuration. In Fig. 6 we compare the ratios of the out-of-band $B(E2;\text{out})$ to in-band $B(E2;\text{in})$ strengths,

$$R_{E2} = B\,(E2;\text{out})/B\,(E2;\text{in})$$

for the γ decays from the γ bands to the ground-state band with the γ decays from bands 17 and 20 to the S band. We assume that the out-of-band $J \rightarrow (J-1)$ transitions are dominated by the $E2$ component due to the $\Delta K = 2$ nature of γ-band to ground-state band transitions [2,55]. It can be seen that these ratios are of the same order of magnitude giving support to the interpretation of the structure of bands 17 and 20. Band 20 crosses the odd-spin γ band between spins 17^+ and 19^+, which will cause some degree of mixing and affect branching ratios and transitions rates. Similarly, there is a mixing of even-spin structures near spin 16^+ that will influence the transition rates from band 17. There is a small signature splitting between bands 17 and 20 with the even-spin states lying lowest in energy. Again, this could either indicate that the S-band configuration is somewhat γ deformed or that these even-spin states mix with nearby states of the same spin and parity. It should be noted that after the alignment of two $i_{13/2}$ neutrons their core has become ^{154}Dy. The γ band in ^{154}Dy shows significant signature splitting [56] also with the even-spin states lying lowest in energy, indicating that it is γ deformed. This shape of the core for the ^{156}Dy S band could be a reason for bands 17 and 20 showing signature splitting.

D. Band 12

Band 12 has no observable signature partner and decays only to the ground-state band with no observed decay branches to other structures. Figure 5(a) shows that band 12 is consistent with a configuration having two aligned $i_{13/2}$ neutrons. An even-spin structure at this excitation energy that has no signature partner could be the S band built on the 0^+_2 second vacuum configuration. This would be the first observation of such a structure. Band 12 has both the correct excitation energy and the correct alignment to support this interpretation. If this is the case, then the plot of the Routhians e' shown in Fig. 5(b) can be used to estimate the crossing frequency [51] $\hbar\omega_c$ of the two bands. The projection of the SV band is found to cross band 12 at $\hbar\omega_c = 0.28(1)$ MeV. The average unattenuated $ABi^2_{13/2}$ aligned S-band crossing in this region of nuclei is $\hbar\omega_c = 0.27(1)$ MeV [52]. This would suggest that this postulated band crossing is not blocked by the nucleons making up the configuration of the second vacuum. As the configuration of the SV band has large components based on the $\nu\{[505]11/2^-\}^2$ configuration and the $[505]11/2^-$ neutrons do not partake in the normal monopole pairing [51], the normal band crossing frequency will not be blocked [52] in agreement with our conjecture.

V. CONCLUSIONS

We have investigated the positive-parity structures in ^{156}Dy at medium spins using the ^{148}Nd(^{12}C,4n) ^{156}Dy reaction at 65 MeV with the Gammasphere spectrometer at the Argonne National Laboratory. Significant extensions have been made for the γ band up to spins 32^+ and 31^+. The new levels that have been established for both even- and odd-spin γ band sequences from the current analysis mark the highest spin ever to be observed for both signatures of a γ band in any nucleus. These bands are also found to faithfully track the ground-state configuration, which is a general feature of γ bands in the transitional rare-earth region.

Three new bands have been discovered, all with an alignment of $\sim 10\hbar$. It is proposed that the even-spin band 17 and the odd-spin band 20 are the even- and odd-spin members of a γ band built on the $i^2_{13/2}$ aligned S band. This is the first example of the observation of γ vibrations built on both the continuation of the ground-state configuration and the aligned S band.

The other newly observed band, band 12, is conjectured to be the $i^2_{13/2}$ aligned S_2 band built on the 0^+_2 second vacuum configuration. The crossing of this band with the band built on the 0^+_2 state is at a rotational frequency of $\hbar\omega_c = 0.28(1)$ MeV, which is consistent with the second vacuum configuration not blocking the monopole pairing.

The new experimental results on γ bands presented here are of particular interest because of new interpretations of $K^\pi = 2^+$ rotational bands in even-even nuclei. In the symplectic shell model [57] $K^\pi = 2^+$ rotational bands arise naturally and are not due to vibrations in the γ degree of freedom. Recent studies

[58] with the algebraic version of the Bohr model, for which calculation without invoking the adiabatic approximation are now feasible, lend strong support for the view [14,49] that low-energy rotational bands are close to being β rigid. It also indicates that they should be near γ rigid as well and that the low-energy $K^\pi = 2^+$ rotational bands are more meaningfully described as rotations with small triaxial deformation of a strongly renormalized SU(3) type.

ACKNOWLEDGMENTS

We would like to thank the crew of the ANL ATLAS accelerator for delivering a very stable and clean beam. The authors also thank the ANL operations staff at Gammasphere and gratefully acknowledge the efforts of J. P. Green for target preparation. In addition we thank D. Radford for software support and S. Åberg for constructive discussions. This work was funded by the U.S. National Science Foundation under Grants No. PHY-1203100 (USNA) and No. PHY-0754674 (FSU) as well as by the U.S. Department of Energy, Office of Nuclear of Nuclear Physics, under Contracts No. DE-AC02-06CH11357 (ANL) and No. DE-FG02-91ER40609 (Yale). One of us J.F.S.-S. would like to thank the Joyce Frances Adlard Cultural Fund for support. S.N.T.M. acknowledges a postgraduate grant from the South African National Research Foundation and thanks the library staff of iThemba LABS for considerable help.

[1] Å. Bohr and B. R. Mottelson, *Nuclear Structure* (World Scientific, Singapore, 1998), Vol. II, p. 363.
[2] K. Schreckenbach and W. Gelletly, Phys. Lett. B **94**, 298 (1980).
[3] A. S. Davydov and G. F. Filippov, Nucl. Phys. **8**, 237 (1958)
[4] L. Wilets and M. Jean, Phys. Rev. **102**, 788 (1956).
[5] G. Gervais *et al.*, Nucl. Phys. A **624**, 257 (1997).
[6] H. H. Schmidt *et al.*, J. Phys. G **12**, 411 (1986).
[7] J. F. Sharpey-Schafer *et al.*, Eur. Phys. J. A **47**, 6 (2011).
[8] J. F. Sharpey-Schafer, S. N. T. Majola, R. A. Bark, T. S. Dinoko, E. A. Lawrie, J. J. Lawrie, S. M. Mullins, J. N. Orce, and P. Papka, PoS **(Bormio2011)** 003.
[9] J Ollier *et al.*, Phys. Rev. C **83**, 044309 (2011).
[10] N. R. Johnson *et al.*, Phys. Rev. Lett. **40**, 151 (1978).
[11] S. W. Yates *et al.*, Phys. Rev. C **21**, 2366 (1980).
[12] J. M. Rees *et al.*, Phys. Rev. C **83**, 044314 (2011).
[13] Jian-Guo Wang *et al.*, Nucl. Phys. A **834**, 94c (2010).
[14] J. F. Sharpey-Schafer *et al.*, Eur. Phys. J. A **47**, 5 (2011).
[15] A. Jungclaus *et al.*, Phys. Rev. C **66**, 014312 (2002).
[16] C. Y. Wu *et al.*, Phys. Rev. C **64**, 064317 (2001).
[17] O. C. Kistner, A. W. Sunyar, and E. der Mateosian, Phys. Rev. C **17**, 1417 (1978).
[18] C. Y. Wu *et al.*, Phys. Rev. C **61**, 021305(R) (2000).
[19] E. Ngijoi-Yogo *et al.*, Phys. Rev. C **75**, 034305 (2007).
[20] D. Ward *et al.*, Nucl. Phys. A **600**, 88 (1996).
[21] D. R. Bès, Mat.-Fys. Medd.-K. Dan. Vidensk. Selsk. **33**(2), 1 (1961).
[22] D. R. Bès, Nucl. Phys. **49**, 544 (1963)
[23] D. R. Bès, P. Federman, E. Maqueda, and A. Zucker, Nucl. Phys. **65**, 1 (1965).
[24] V. G. Soloviev, Nucl. Phys. **69**, 1 (1965).
[25] F. A. Gareev *et al.*, Sov. J. Part. Nucl. **4**, 148 (1973).
[26] F. Iachello, Phys. Rev. Lett. **85**, 3580 (2000).
[27] E. A. McClutchan *et al.*, Phys. Rev. C **76**, 024306 (2007).
[28] E. R. Marshalek and J. Wesner, Phys. Rev. C **2**, 1682 (1970).
[29] E. S. Hernández and A. Plastino, Z. Phys. **268**, 337 (1974); Z. Phys. A **273**, 273 (1975).
[30] J. L. Egido, H. J. Mang, and P. Ring, Nucl. Phys. A **339**, 390 (1980).
[31] Y. R. Shimitzu and K. Matsuyanagi, Prog. Theor. Phys. **72**, 799 (1984).
[32] K. Hara and Y. Sun, Int. J. Mod. Phys. E **04**, 637 (1995).
[33] J. A. Sheikh and K. Hara, Phys. Rev. Lett. **82**, 3968 (1999).
[34] Yang Sun *et al.*, Phys. Rev. C **61**, 064323 (2000).
[35] J. A. Sheikh *et al.*, Phys. Rev. C **77**, 034313 (2008)
[36] J. A. Sheikh *et al.*, Nucl. Phys. A **824**, 58 (2009).
[37] I. Y. Lee, Nucl. Phys. A **520**, c641 (1990).
[38] D. C. Radford, Nucl. Instrum. Methods Phys. Res., Sect. A **361**, 297 (1995).
[39] K. S. Krane, R. M. Steffen, and R. M. Wheeler, Nucl. Data Tables **11**, 351 (1973).
[40] P. J. Twin, Nucl. Instrum. Methods **106**, 481 (1973).
[41] P. A. Butler, P. E. Carr, L. L. Green, A. N. James, P. J. Nolan, J. F. Sharpey-Schafer, P. J. Twin, and D. A. Viggars, Nucl. Instrum. Methods **108**, 497 (1973).
[42] S. N. T. Majola, M.Sc. thesis, University of Cape Town, 2011.
[43] F. G. Kondev *et al.*, Phys. Lett. B **437**, 35 (1998).
[44] M. A. Caprio *et al.*, Phys. Rev. C **66**, 054310 (2002).
[45] M. A. Riley *et al.*, Nucl. Phys. A **486**, 456 (1988).
[46] H. R. Andrews, D. Ward, R. L. Graham, and J. S. Geiger, Nucl. Phys. A **219**, 141 (1974).
[47] W. D. Kulp *et al.*, Phys. Rev. C **76**, 034319 (2007).
[48] I. Ragnarsson and R. A. Broglia, Nucl. Phys. A **263**, 315 (1976).
[49] J. F. Sharpey-Schafer, in *Proc. Int. African Symp. On Exotic Nuclei IASEN2013, Somerset-West, South Africa, 2013*, edited by E. Cherepanov *et al.* (World Scientific, Singapore, 2015), p. 451.
[50] S. Y. Chu, J. O. Rasmussen, M. A. Stoyer, P. Ring, and L. F. Canto, Phys. Rev. C **52**, 1407 (1995).
[51] J. D. Garrett *et al.*, Phys. Lett. B **118**, 297 (1982).
[52] J. D. Garrett *et al.*, Phys. Rev. Lett. **47**, 75 (1981).
[53] R. Bengtson and S. Frauendorf, Nucl. Phys. A **314**, 27 (1979).
[54] L. L. Riedinger *et al.*, Phys. Rev. Lett. **44**, 568 (1980).
[55] I. Alfter, E. Bodenstedt, W. Knichel, and J. Schüth, Nucl. Phys. A **635**, 273 (1998).
[56] D. R. Zolnowski, M. B. Hughes, J. Hunt, and T. T. Sugihara, Phys. Rev. C **21**, 2556 (1980).
[57] J. Carvalho, R. Le Blanc, M. Vasanji, D. J. Rowe, and J. B. McGrory, Nucl. Phys. A **452**, 240 (1986).
[58] D. J. Rowe (private communication).